A Solid-State, Solution, and Theoretical Structural Study of Kinetic and Thermodynamic Lithiated Derivatives of a Simple Diazomethane and Their Reactivities Towards Aryl Isothiocyanates

David R. Armstrong,*[a] Robert P. Davies,[b] Robert Haigh,[c] Mark A. Hendy,[c] Paul R. Raithby,[d] Ronald Snaith,[†] and Andrew E. H. Wheatley*[c]

Dedicated to the memory of Ron Snaith

Keywords: Density functional calculations / Diazomethane / Lithium / Solid-state structures / Solution structure

(Trimethylsilyl)diazomethane (**1-H**) reacts with *n*BuLi in THF at elevated temperature to afford (previously reported) **1-Li·$^3/_2$THF**. However, reaction in hexane/TMEDA at low temperature affords instead the *N*-lithiate $Me_3SiCNNLi$·TMEDA (**9**), which is a novel "open" pseudo-cubic tetramer in the solid state. Variable-temperature NMR spectroscopy suggests that *N*-metallated **9**, apparently the kinetic product of the reaction, irreversibly rearranges at high temperature in solution to give the thermodynamically preferred *C*-lithiated isomer. These observations, supported by DFT calculations, influence our understanding of the reactivity of lithiated diazomethanes towards aryl isothiocyanates, suggesting as they do that previously observed product selectivity in these reactions is critically dependent on temperature control exercised during the process.

Introduction

(Trimethylsilyl)diazomethane (**1-H**), a safe and stable analogue of diazomethane, has many applications in, for example, Arndt−Eistert syntheses,[1] the homologation of ketones[2] and aldehydes,[3] cycloaddition reactions,[4] and the methyl esterification of carboxylic acids.[5] Moreover, the chemistry of its lithiated derivative (**1-Li**) has also been extensively studied due to its synthetic utility. This derives from its combination of reactivity (greater than that of **1-H**) and safety (relative to diazomethane).[6] In consequence, **1-Li** has found ready use in the preparation of substituted triazoles[7] and tetrazoles,[8] the syntheses of aldehydes from ketones,[9] Colvin rearrangements[10] and the formation of synthetically useful[11] silyl ketenes.[12] These last species react with phosphorus ylides and so afford a simple route to silyl allenes.[13] In this context, central to the synthesis[13] of the disubstituted silyl ketene **3**, is the formation, by the sequential treatment of **1-H** with *n*-butyllithium and carbon monoxide, of a lithium ynolate **2**. This latter species is considered to result from the insertion[14] of CO into the proposed C−Li bond in **1-Li**, whereupon N_2 is eliminated (Scheme 1), the addition of triethylsilyl trifluoromethanesulfonate (Et_3SiOTf) and subsequent work-up affording **3**.

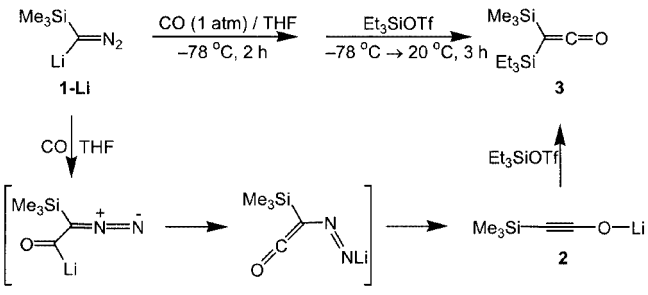

Scheme 1. Proposed mechanism for the preparation of the disubstituted silyl ketene **3**[13]

[a] Department of Pure and Applied Chemistry, University of Strathclyde,
295 Cathedral Street, Glasgow, G1 1XL, U. K.
Fax: (internat.) +44-141/548-4822
E-mail: drarmstrong@strath.ac.uk
[b] Department of Chemistry, Imperial College London,
South Kensington, London, SW7 2AZ, U. K.
Fax: (internat.) +44-20/7594-5804
E-mail: r.davies@imperial.ac.uk
[c] Department of Chemistry, University of Cambridge,
Lensfield Road, Cambridge, CB2 1EW, U. K.
Fax: (internat.) +44-1223/336-362
E-mail: rh293@cam.ac.uk, aehw2@cam.ac.uk
[d] Department of Chemistry, University of Bath,
Claverton Down, Bath, BA2 7AY, U. K.
Fax: (internat.) +44-1225/386-231
E-mail: p.r.raithby@bath.ac.uk
Supporting information for this article is available on the WWW under http://www.eurjic.org or from the author.
[†] Deceased.

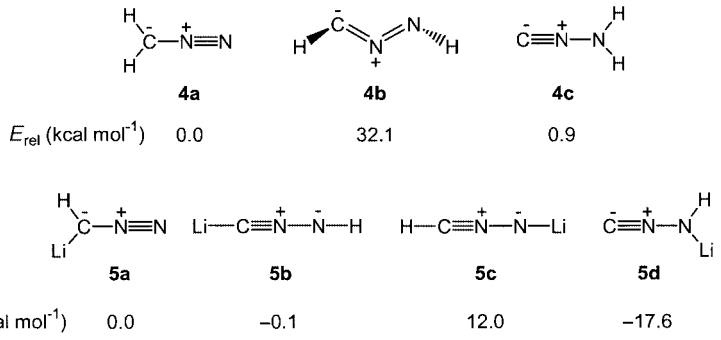

Figure 1. Possible isomers of **1-H**[15] (and their relative energies)[17] and **1-Li** (and their relative energies, 1 kcal = 4.184 kJ)

The chemistry of metallated (mono-substituted) diazomethane has been previously investigated[15] (Figure 1) with results indicating that deprotonation/reprotonation of diazomethane **4a** affords the *less* stable CH_2N_2 *N*-isocyanoamine isomer **4c**, which undergoes base-induced reversion to **4a**. The other possible non-cyclic CH_2N_2 isomer (nitrile imine **4b**) has not been detected experimentally. The structures and energies of the CH_2N_2 isomers **4a**−**c**, as well as those of their lithiated derivatives, **5a**−**d**, have recently been modelled theoretically.[16,17] From these calculations it was suggested that while N-protonation of **5d** would give **4c**, C-protonation of **5a** would yield **4a**. Further, consistent with experiment, theory pointed to the most stable **1-H** isomer (**4a**) being obtainable, in the presence of base, from energetically less favourable **4c** (Scheme 2). This is in spite of the suggestion, based on calculation, that **5a** (precursor to **4a**) is less stable than **5d**; in other words that the reaction is thermodynamically controlled by the stability of the final protonated product. In contrast to the parent diazomethane structures discussed above, calculations[17] have shown that for the lithiated mono-substituted (trimethylsilyl)diazomethanes **1-Li** and **6** (Figure 2), the *N*-metallated nitrile imine isomer was slightly more stable than the *C*-lithiate. However, previous attempts to isolate and crystallographically characterise **6** have resulted only in the isolation and structural elucidation of {hexakis[lithio(trimethylsilyl)-diazomethane]·bis[lithio{4,5-bis(trimethylsilyl)triazole}]·heptakis(diethyl ether)} [(**7**)$_2$·OEt_2; Figure 3].[17] This species is composed both of **6** and lithiotriazole **8**, this last component evidently being formed by the reaction of **6** with **1-H**.

Suggestions[12,18] that the reactivity of lithiated **1-H** is solvent dependent have been borne of the observation that whereas it reacts with RNCS (R = alkyl, aryl) in OEt_2 to afford 2-amino-1,3,4-thiadiazole (**13**), in THF thio-1,2,3-triazoles **10**−**12** result (Scheme 3).[18b] However, such differing behaviour has not hitherto been explained in detail and this has led us to attempt the isolation and structural characterisation of *pure* lithiated (trimethylsilyl)diazomethane (cf. **7**) in order to clarify which of the proposed model structures, *C*- or *N*-lithiated, better describes the true structure of lithiated **1-H**. In this context, we report here on the observation of both kinetic [giving $Me_3SiCNNLi$·TMEDA, **9**] and thermodynamic [giving **1-Li·$^3/_2$THF**] metallation. The latter observation has led to the isolation and structural characterisation of an intermediate in the synthesis of disubstituted silyl ketene **3** (Scheme 1). Finally, we report here on the reactions of lithiodiazomethanes with different isothiocyanates with a view to understanding the relationship between the site of lithiation in the substrate and the structure of the final cyclised product.

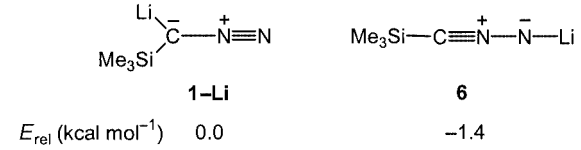

Figure 2. *C*- and *N*-lithiated isomers of **1-Li** and their relative energies[17]

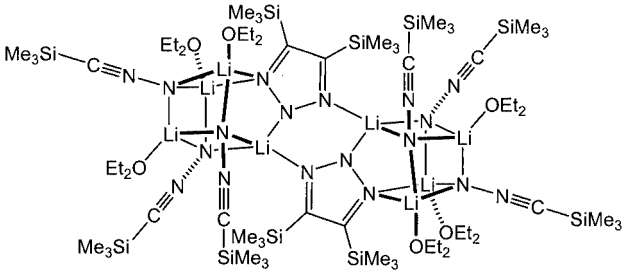

Figure 3. The molecular structure of (**7**)$_2$

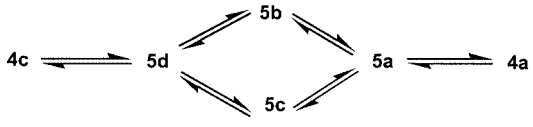

Scheme 2. Equilibria in the interconversion of diazomethane isomers

Results and Discussion

Solid-State and Theoretical Studies on 1-Li·$^3/_2$THF and 9

The reaction of **1-H** with *n*BuLi in THF yielded large yellow crystals of pure lithiated (trimethylsilyl)diazomethane $^1/_2$[{$Me_3SiC(Li)N_2$}$_2$·3THF] (**1-Li·$^3/_2$THF**), the solid-state structure of which we have previously reported.[19] X-

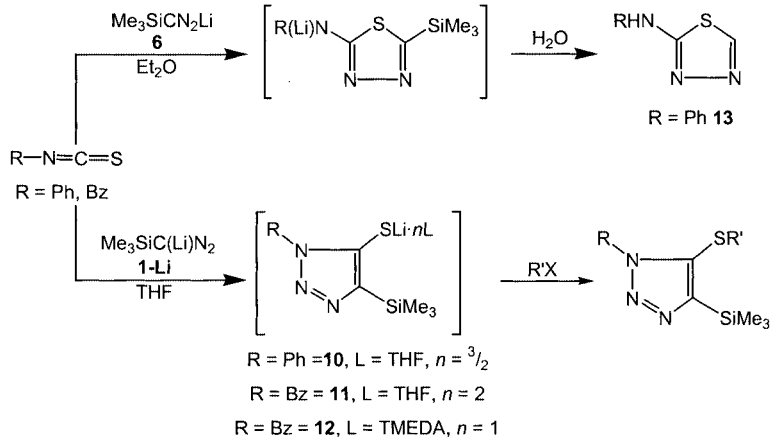

Scheme 3. Proposed pathways for the reaction of different **1-Li** isomers with RNCS (R = Ph, Bz)[12,18]

ray crystallography has shown **1-Li·$^3/_2$THF** to be a polymer based on a repeating tetramer unit (Figure 4), consisting of two (*mono*-THF) complexed lithiodiazomethane molecules and two (*bis*-THF) complexed ones i.e. $\{[Me_3SiC(Li{\cdot}THF)N_2]{\cdot}[Me_3SiC(Li{\cdot}2THF)N_2]\}_2$. This revelation of two types of lithiodiazomethane molecule in the solid-state structure of **1-Li·$^3/_2$THF** is consistent with the observation of two sets of C=N=N stretching modes by IR spectroscopy (ν_{sym} = 2149, 2116 cm^{-1} and ν_{asym} = 2092, 2052 cm^{-1}) which collapse to a single set upon hydrolysis to **1-H**. The ambiguity surrounding the preferred site of lithiation in **1-H** that results from the contrasting structures noted for **1-Li·$^3/_2$THF** and **7** made it desirable to theoretically probe the relative stabilities and geometries of both *N*- and *C*-lithiates. DFT calculations[20] based on a variety of models were undertaken (B3LYP[21]/6-311G**[22]). Energetic results for $XCN_2Li{\cdot}nL$ (X = H_3Si, Me_3Si; n = 0, 1, 2; L = OEt_2, THF) are summarised in Table 1 with selected calculated geometrical parameters in Table E1 (see Electronic Supporting Information; see footnote on the first page of this article).

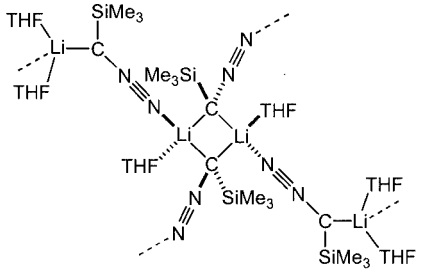

Figure 4. The molecular structure of polymeric **1-Li·$^3/_2$THF**

Overall, calculations reported here on lithiodiazomethanes and their complexes suggest that, while *N*-metallation is thermodynamically preferred, *C*-metallation becomes increasingly favourable in the presence of strongly coordinating media. For unsolvated diazomethanes XCN_2Li (X = H_3Si, Me_3Si) *C*-lithiation is 2.5 kcal·mol^{-1} (**I**; 1 kcal = 4.184 kJ) more energetic than *N*-lithiation (**II**) for X = H_3Si (Table 1 and Figure 5) while for X = Me_3Si the computed preference for *N*- (**IV**) over *C*-metallation (**III**) is 4.0 kcal·mol^{-1}, illustrating the electron-donating nature of the methyl groups over hydrogen atoms yet still suggesting a fine energetic balance between the differently metallated, unsolvated monomers. Calculated molecular geometries show little dependence upon X. Whereas *C*-lithiates **I** and **III** both show relatively long C−N (1.283 and 1.282 Å, respectively) and short N−N (1.141 and 1.144 Å, respectively) bonds, the opposite is true of *N*-lithiates **II** and **IV** (C−N = 1.195 Å in both, N−N = 1.201 and 1.205 Å, respectively). The structural feature most significantly dependent on X is the Si−C bond length. This increases significantly from a mean of 1.798 Å to one of 1.817 Å on replacing H atoms with Me groups−presumably reflecting both the increased steric requirements of the trimethylsilyl group and its aforementioned inductive effect. The metallo−organic bonds show no significant variation with X. Hence, while the C−Li bonds are 1.906 Å in both **I** and **III**, the N−Li ones in **II** and **IV** are 1.697 and 1.692 Å, respectively.

The extension of calculations to the simple mono-solvated, monomeric lithiates $Me_3SiCN_2Li{\cdot}L$ (L = OEt_2, THF) shows that, irrespective of the choice of L, the *C*-lithiates (**V**, **VII**) are higher in energy than the *N*-lithiates (**VI**, **VIII**; Table 1 and Figure 5). All of the resultant structure types are significantly more stable than either **III** or **IV** by virtue of Lewis base coordination [$\Delta E_{Complexation}$ (ΔE_C) = −21.5 (**V**), −22.9 (**VII**), −21.5 (**VI**), −22.7 (**VIII**) kcal·mol^{-1}]. Of note (see below) for both types of L, *C*-lithiated models show more negative ΔE_C values than their *N*-lithiated counterparts. Moreover, for both *C*- and *N*-lithiates, both the magnitude of and differences between ΔE_C values are enhanced for coordination of the stronger Lewis base (THF). Thus, $-\Delta E_C$(**V**) = $-\Delta E_C$(**VI**) and $-\Delta E_C$(**VII**) > $-\Delta E_C$(**VIII**), $-\Delta E_C$(**VII**) > $-\Delta E_C$(**V**) and $-\Delta E_C$(**VIII**) > $-\Delta E_C$(**VI**) and, whereas for *mono*-OEt_2 solvation **VI** is preferred to **V** by 4.0 kcal·mol^{-1}, for *mono*-THF solvation **VII** is 3.8 kcal·mol^{-1} more stable than **VIII**. This implies that *N*-metallation is less strongly favoured over *C*-metal-

Table 1. Summary of DFT calculations (B3LYP/6-311G**)[21,22] based on $XCN_2Li{\cdot}nL$ (X = H_3Si, Me_3Si; n = 0, 1, 2; L = OEt_2, THF, TMEDA). (1 kcal = 4.184 kJ.) ΔE_c/L quoted as enthalpy of complexation per Lewis base *donor atom*

Model	Figure	Formula	Total Energy (incl. ZPE; Hartrees)	ΔE_c (kcal mol^{-1})	ΔE_c/L (kcal mol^{-1} L^{-1})	Relative Energy (kcal mol^{-1} L^{-1})
I	E1	$H_3SiC(Li)N_2$	−446.410355	–	–	2.5
II	E1	H_3SiCN_2Li	−446.414282	–	–	0.0
III	E1	$Me_3SiC(Li)N_2$	−564.343445	–	–	4.0
IV	E1	Me_3SiCN_2Li	−564.349859	–	–	0.0
V	E1	$Me_3SiC(Li{\cdot}OEt_2)N_2$	−797.976187	−21.5	−21.5	4.0
VI	E1	$Me_3SiCN_2Li{\cdot}OEt_2$	−797.982585	−21.5	−21.5	0.0
VII	E1	$Me_3SiC(Li{\cdot}THF)N_2$	−796.779249	−22.9	−22.9	3.8
VIII	E1	$Me_3SiCN_2Li{\cdot}THF$	−796.785302	−22.7	−22.7	0.0
IX	E2	$Me_3SiC(Li{\cdot}2OEt_2)N_2$	−1031.594155	−33.7	−16.9	3.0
X	E2	$Me_3SiCN_2Li{\cdot}2OEt_2$	−1031.598894	−32.6	−16.3	0.0
XI	E2	$Me_3SiC(Li{\cdot}2THF)N_2$	−1029.205798	−40.1	−20.1	2.6
XII	E2	$Me_3SiCN_2Li{\cdot}2THF$	−1029.209892	−38.7	−19.3	0.0
XIII	E2	$Me_3SiC(Li{\cdot}TMEDA)N_2$	−912.022702	−35.1	−17.6	1.7
XIV	E2	$Me_3SiCN_2Li{\cdot}TMEDA$	−912.025424	−32.8	−16.4	0.0

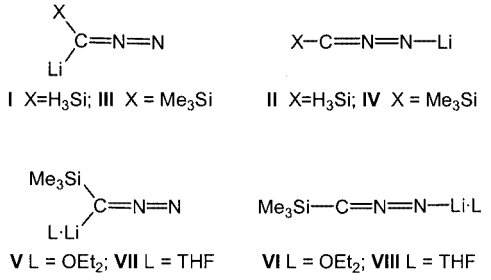

Figure 5. Theoretically modelled structures of the simple *C*- (**I**, **III**) and *N*-lithiated (**II**, **IV**) diazomethanes XCN_2Li (X = H_3Si, Me_3Si) and **III**·L and **IV**·L complexes (**V**−**VIII**; L = OEt_2, THF)

lation as external solvation increases; an important inference given the previously reported reactivities of lithiated (trimethylsilyl)diazomethanes in different Lewis base media.[12,18] Differences in the calculated energies of the variously coordinated *mono*-solvates do not, however, translate into significant differences in bonding parameters. Slight changes are noticeable relative to unsolvated **III** and **IV** on the inclusion of Lewis base and this is most apparent in increments to C−Li lengths (to, 1.959 and 1.956 Å for **V** and **VII**, respectively, cf. 1.906 Å in **III**) and N−Li distances (to, 1.735 and 1.732 Å for **VI** and **VIII**, respectively, cf. 1.692 Å in **IV**).

Calculations on $Me_3SiCN_2Li{\cdot}2$ L (L = OEt_2, THF; Table 1 and Figure 6) reinforce the view that, irrespective of the choice of L, the preference for *N*- over *C*-lithiation is diminished as external solvation of the metal is introduced. The resultant structure types (**IX**−**XII**) are all significantly more stable than models **V**−**VIII** [ΔE_C = −33.7 (**IX**), −40.1 (**XI**), −32.6 (**X**), −38.7 (**XII**) kcal·mol^{-1}]. As for **V**−**VIII**, ΔE_C is most negative for solvation by THF while the predilection for *N*-metallation is minimised in this medium [$Me_3SiC(Li{\cdot}2THF)N_2$ (**XI**) is only 2.6 kcal·mol^{-1} less stable than $Me_3SiCN_2Li{\cdot}2THF$ (**XII**)]. The addition of a second Lewis base molecule causes the further extension of C−Li (to, 2.055 and 2.038 Å for **IX** and **XI**, respectively) and N−Li bonds (to 1.801 Å for both of **X** and **XII**).

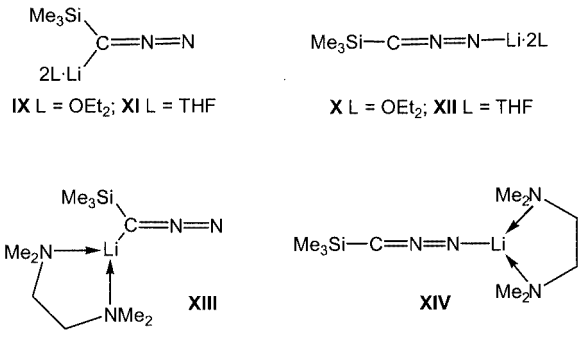

Figure 6. Modelled structures of monomeric **III**·2L and **IV**·2L complexes **IX**−**XII**; L = OEt_2, THF) and **III**·L and **IV**·L (L = TMEDA)

While the gas phase calculations do not account for the aggregation behaviour either of **1-Li·$^3/_2$THF** or of **7** it is nonetheless apparent that some useful correlations exist between theory and experiment. Table E1 (Supp. Inf.) indicates close carbon−nitrogen and the nitrogen−nitrogen bond length agreement both between **1-Li·$^3/_2$THF** and **I** (Figure 5) and between **7** and **II**. Clearly, in **1-Li·$^3/_2$THF** the carbon−nitrogen bond (mean 1.326 Å) is longer than a double one and the nitrogen−nitrogen bond (1.182 Å) is shorter than a double one.[23] Furthermore in **7**, the

carbon−nitrogen bond (mean 1.202 Å) is longer than a triple one and the nitrogen−nitrogen bond (1.208 Å) is slightly longer than a double one.

Previously reported calculations on H_3SiCN_2Li [6-31G(d)/MP2] have suggested (in the light of structurally characterising **7**) an energetic preference of 1.4 kcal·mol^{-1} for the *N*- over the *C*-lithiate.[17] However, calculations presented here clearly suggest that any such preference is eroded by the introduction of external solvation. This leads us to the view that in the presence of excess donor (either solvent or, by aggregation, other molecules of lithiated **1-H**) the *C*-metallated product represents the thermodynamic product of lithiation whereas the *N*-metallate reveals kinetic control. Consistent with this is the fact that, whereas **1-Li·$^3/_2$THF** is afforded after having heated the reaction mixture to reflux (approx. 65 °C), **7** results from a process in which the temperature never exceeds −25 °C.

In order to further probe the question of thermodynamic versus kinetic control in the metallation of **1-H** and also in an attempt to obtain pure lithiated derivatives based on oligo- rather than complex polymeric structures, we have effected the crystallisation of lithiated (trimethylsilyl)diazomethanes from polydentate Lewis bases. The best results have been obtained by the reaction of **1-H** with *n*BuLi in TMEDA (= *N*,*N*,*N*′,*N*′-tetramethylethylenediamine) at low temperature (< −25 °C). This process achieves yellow crystals of a single isolable product and these analyse as Me_3SiCN_2Li·TMEDA (**9**). Not only does ^{1}H NMR spectroscopy support the 1:1 TMEDA/lithiate ratio but it also, by displaying just a single trimethylsilyl resonance, suggests the adoption of a single aggregation state, symmetrical species in solution. In line with the kinetic control exercised during the reaction, the solid-state structure of **9** reveals a tetramer (Table 2 and Figures 7 and 8) consisting of *N*-lithiated (trimethylsilyl)diazomethane molecules arranged as an "open" pseudo-cubane. Unusually, stabilisation of the metal centres by TMEDA takes two distinct forms with both *mono*- and *bi*dentate coordination modes being observed. Notably, such a structure is incompatible with the symmetry suggested by NMR spectroscopy, suggesting that the structure is either rapidly fluxional and/or significantly deaggregated in solution (see below).

While Li(1), Li(2), and Li(4) are each coordinated by three diazomethane terminal N-centres, Li(3) is coordinated by just two; there being no interaction with N(1) [Li(3)···N(1) = 2.839(9) Å]. *Bis*-coordination by the two TMEDA molecules that exhibit bidentate behaviour renders Li(3) and Li(4) four and five coordinate, respectively. The remaining two Li^+ ions are tetra-coordinate, each being *mono complexed* by one N-centre of a monodentate TMEDA molecule. Thus the aggregate can be viewed as a dimer of dimeric pairs [each one based on a $(NLi)_2$ ring, i.e. Li(3)N(5)Li(4)N(7) and Li(1)N(1)Li(2)N(3)] whereby each one is defined by the characteristic behaviour of its TMEDA components (Figure 8). Nevertheless, the combination of pseudo-cubane opening and differences in the coordinative modes adopted by TMEDA incurs significant variations in core Li−N interactions (Table 2). Perhaps most significantly, and presumably symptomatic of the predilection of lithium for forming four bonds,[24] pentacoordinate Li(4) forms long[25] interactions both with bidentate TMEDA [mean Li(4)−N = 2.264 Å] and with three deprotonated diazomethane monomers [mean Li(4)−N = 2.204

Table 2. Selected bond lengths [Å] and angles [°] in **9**

Li(1)−N(1)	1.991(7)	Li(4)−N(5)	2.211(8)
Li(1)−N(3)	2.108(7)	Li(4)−N(7)	2.288(8)
Li(1)−N(7)	2.045(8)	Li(4)−N(15)	2.324(8)
Li(1)−N(9)	2.067(7)	Li(4)−N(16)	2.203(8)
Li(2)−N(1)	2.010(7)	N(1)−N(2)	1.204(5)
Li(2)−N(3)	2.042(7)	N(2)−C(1)	1.210(6)
Li(2)−N(5)	2.046(7)	N(3)−N(4)	1.216(5)
Li(2)−N(11)	2.091(7)	N(4)−C(5)	1.212(6)
Li(3)−N(5)	2.058(8)	N(5)−N(6)	1.219(5)
Li(3)−N(7)	2.011(7)	N(6)−C(9)	1.209(6)
Li(3)−N(13)	2.208(9)	N(7)−N(8)	1.218(5)
Li(3)−N(14)	2.146(8)	N(8)−C(13)	1.193(6)
Li(4)−N(3)	2.113(8)		
N(1)−Li(1)−N(3)	97.4(3)	N(3)−Li(2)−N(5)	97.1(3)
Li(1)−N(1)−Li(2)	81.9(3)	Li(2)−N(3)−Li(4)	135.6(3)
Li(1)−N(3)−Li(2)	78.4(3)	Li(2)−N(5)−Li(4)	84.8(3)
N(1)−Li(2)−N(3)	98.9(3)	N(3)−Li(4)−N(5)	90.3(3)
N(3)−Li(1)−N(7)	97.0(3)	N(5)−Li(3)−N(7)	98.4(3)
Li(1)−N(3)−Li(4)	87.9(3)	Li(3)−N(5)−Li(4)	86.8(3)
Li(1)−N(7)−Li(4)	84.8(3)	Li(3)−N(7)−Li(4)	85.8(3)
N(3)−Li(4)−N(7)	89.9(3)	N(5)−Li(4)−N(7)	86.4(3)

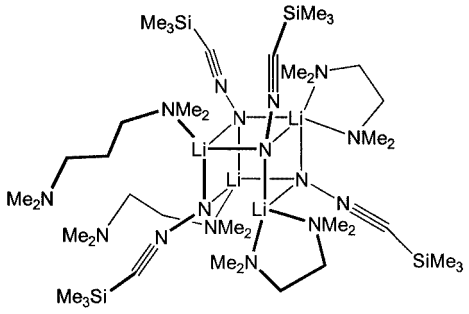

Figure 7. The molecular structure of $(\mathbf{9})_4$

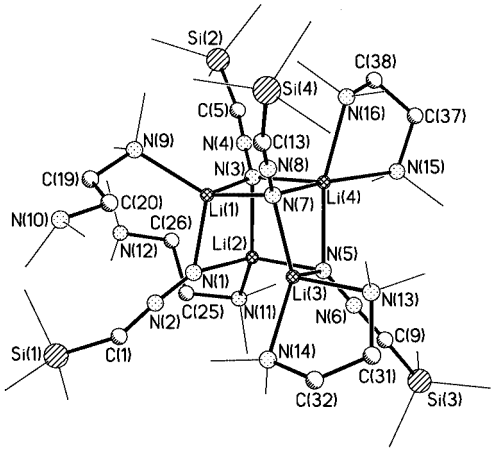

Figure 8. Solid-state structure of tetrameric **9**; hydrogen atoms and minor disorder omitted for clarity

Å]. The remaining TMEDA-chelated metal shows similar, though less pronounced, lengthening of Li−N(TMEDA) bonds [Li(3)−N(13) and Li(3)−N(14) = 2.208(9) and 2.146(8) Å, respectively] but rather stronger bonds to the cluster core [mean Li(3)−N = 2.035 Å]. It may be the case that the discrepancy between these two Li−N(TMEDA) interactions has its origins in the orientation of the Lewis base since the shorter of the two interactions is associated with N(14), which can presumably closely approach Li(3) by virtue of diminished steric interactions with the N(1)-containing diazomethane unit−a result of the extended Li(3)···N(1) distance. A further consequence of bond-cleavage in the aggregate core is that N(1) becomes unique among the terminal diazomethane N-centres in that it stabilises just two metal ions [mean Li−N(1) = 2.001 Å]. Finally, shorter than the Li−N(TMEDA) bonds previously noted for the *bis*-coordinating Lewis base molecules are those in which the TMEDA acts only as a monodentate donor [mean Li−N = 2.079 Å]. A comparison of the solid-state structural parameters observed for **9** with those noted in **7** reveals that both C−N (mean 1.206 and 1.202 Å respectively for **9** and **7**) and N−N (mean 1.214 and 1.208 Å) bond lengths correlate well but differ significantly from those in *C*-lithiated **1-Li·$^3/_2$THF**.[19]

Coincidentally, the only other known example of an "open" $(LiN)_4$ pseudo-cubane in which a single core bond is absent is **7**. However, bond cleavage in **7** derives from the mixed-anion nature of the cluster, with one vertex of the [otherwise lithio(trimethylsilyl)diazomethane-based] cube being defined by the deprotonated N-centre in the triazole ring, the neighbouring ring-nitrogen inserting into a cubane edge. The only other discrete, related "open" pseudo-cubanes reported are the $(LiO)_4$-based structures $(PhOLi{\cdot}THF)_4{\cdot}PhOH$ (wherein a single core interaction is absent),[26] $[2\text{-}MeOC_6H_4C(H)(OLi)NMe(CH_2)_2NMe_2]_4$[27] and $[PhC(O)N(Ph)Li{\cdot}THF]{\cdot}[PhC(O)N(Ph)Zn(t\text{Bu})_2\text{-}Li{\cdot}THF]$[28] (in each of which two eclipsed core bonds are absent). This latter mode of separation is also noted in polymeric $(BrLi{\cdot}THF)_\infty$.[29] The remaining rare feature of $(\mathbf{9})_4$ in the solid state is highlighted by $Cl_6Li_6{\cdot}2TMEDA{\cdot}{}^4/_2TMEDA$.[30] Here variations in the mode of external solvation by TMEDA allow four of the six Lewis base molecules associated with each hexamer to bridge between aggregates affording a three-dimensional network. Contrastingly, in $(\mathbf{9})_4$, Li(1) and Li(2) are each stabilised by just one TMEDA N-centre [N(9), N(11)]; these donors being strictly monodentate with neither N(10) nor N(12) bridging to adjacent aggregates.

Complex **9** (like **7**) results from the employment of kinetic control during the reaction and this, perhaps, overshadows the true aim of employing TMEDA here. Nevertheless, the solid-state structure of **9** affords us the first glance of a discrete molecular lithiodiazomethane [cf. $(\mathbf{1\text{-}Li\cdot{}^3/_2THF})_\infty$] which incorporates no other by-products (cf. **7**) and a theoretical probe has been undertaken [B3LYP/6-311G**;[21,22] Figure 6 and Table 1 and Table E2 (Supp. Inf.)].[20−22] The stabilities of $Me_3SiC(Li{\cdot}TMEDA)N_2$ (**XIII**) and $Me_3SiCN_2Li{\cdot}TMEDA$ (**XIV**) are significantly enhanced by the coordination of TMEDA [ΔE_C = −35.1 (**XIII**), −32.8 (**XIV**) kcal·mol^{-1}] relative to unsolvated **III** and **IV**. In line with earlier calculations reported here (see above) $-\Delta E_C$(**XIII**) > $-\Delta E_C$(**XIV**), pointing again to the chances of *C*-metallation being enhanced by external solvation. Whilst *C*-lithiate **XIII** is still less stable than *N*-lithiated analogue **XIV** the introduction of TMEDA has almost completely negated the energy difference (1.7 kcal·mol^{-1}). The structural parameters in diazomethane anions in **9** correlate well with those of computed **XIV**. Notably, in **9** (as in **7**) the carbon−nitrogen and the nitrogen−nitrogen bond lengths are very similar (in contrast to those in *C*-lithiated **1-Li·$^3/_2$THF**, wherein the carbon−nitrogen distance was significantly greater than the nitrogen−nitrogen one).

Solution Studies on 1-Li·$^3/_2$THF and 9

The observation of **1-Li·$^3/_2$THF** and **9** demonstrates the viability of both *C*- and *N*-lithiated derivatives of **1-H** in the solid state. However, the details of their syntheses suggest that the regiospecificity of metallation is critically dependant on reaction conditions. This observation made it desirable to elucidate the structures of species obtained on dissolution of both **1-Li·$^3/_2$THF** and **9** and to probe the possible interconversion between *N*- and *C*-lithiates. Cryoscopic relative molecular mass (CRMM) measurements[31] on **1-Li·$^3/_2$THF** in benzene show both that the complex deaggregates significantly in non-donor solution and that the molecular mass (M_r) and aggregation state (n) remain essentially constant at 177 ± 10 and n = 0.77 ± 0.04, respectively [assuming n = 1 for $Me_3SiC(Li)N_2{\cdot}{}^3/_2THF$, M_r = 228] over a wide concentration range ($4.55{\cdot}10^{-3}$ to $3.20{\cdot}10^{-2}$ mol·dm^{-3}, Table E3, Supp. Inf.). This may signify the polymer (M_r = 912) breaking down (the chain-linking Li−N bonds cleaving) such that $[Me_3SiC(Li{\cdot}THF)N_2]_2$ dimers (M_r = 384) and $Me_3SiC(Li{\cdot}2THF)N_2$ monomers (M_r = 264) result. Dimerisation of these monomers, concomitant with the evolution of THF molecules yields fundamental *mono*-THF solvated dimers in solution (M_r = 228). Deaggregation of — and/or loss of THF from — these species can then explain the observed M_r. For **9**, CRMM measurements suggest significant deaggregation of the tetramer. Over the concentration range $4.80{\cdot}10^{-2}$ to $2.60{\cdot}10^{-1}$ mol·dm^{-3} (Table E4, Supp. Inf.) M_r increases from 425 ± 5 (n = 1.80 ± 2 assuming n = 1 for $Me_3SiCN_2Li{\cdot}TMEDA$) to 494 ± 3 (n = 2.14 ± 2). This points to substantial dislocation of the tetramer (M_r = 945) to give $(Me_3SiCN_2Li{\cdot}TMEDA)_2$ (M_r = 473), with limited dissociation of dimers and/or de-coordination of TMEDA occurring at lower concentrations. Data indicates some tetramer retention at higher concentrations.

Variable-temperature ^{1}H NMR spectra of **9** in $[D_8]$PhMe (Figure 9) reveal broadening of the TMEDA peaks and downfield movement of the Me_3Si signal as the temperature is reduced. By −25 °C new sets of Me_3Si and (both) TMEDA resonances develop, suggesting the evolution of a second species and, as the temperature is further reduced, these new signals become dominant. Such behaviour is consistent with the aggregation of $(Me_3SiCN_2Li{\cdot}TMEDA)_2$

(see above) to give tetramers at low temperature and, as such, these spectral changes are thermally reversible. If, instead, this sample is heated above room temperature the Me_3Si singlet (δ = 0.28 ppm at 35 °C) is replaced by a second one (δ = 0.34 ppm at 52 °C; both signals are present in the range 45−51 °C) suggesting a significant change in the lithiodiazomethane molecule whereby kinetically favoured *N*-lithiate **9** rearranges to the (thermodynamic) *C*-lithiate in situ. This view is supported by the observation that subsequent cooling of the sample to room temperature fails to incur any further significant changes in the appearance of the spectrum, suggesting that this thermal rearrangement is irreversible.

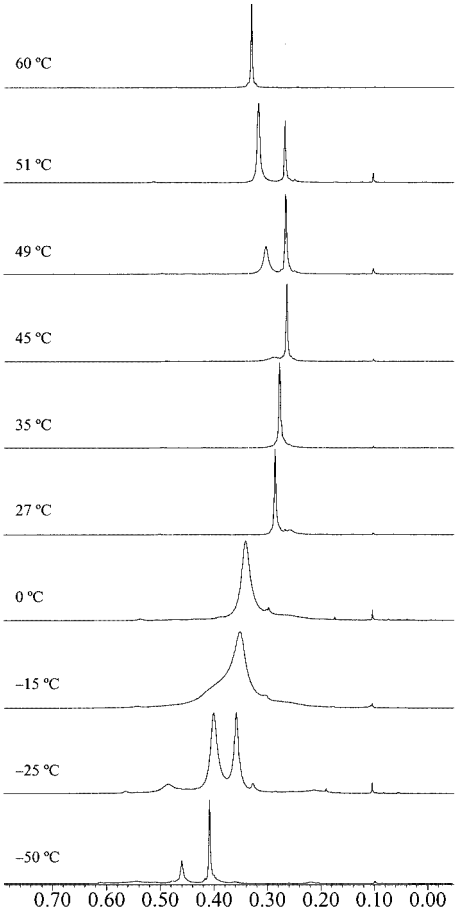

Figure 9. ^{1}H NMR spectroscopic data for the Me_3Si group in **9** in [D_8]PhMe over the range 60 °C to −50 °C

The room temperature ^{13}C NMR spectrum of **9** in [D_8]PhMe (Figure 10) shows a dominant Me_3Si signal at δ = 2.2 and a significantly smaller one at δ = −0.8. (This latter signal may represent a small amount of the sample converting slowly to the thermodynamic isomer at room temperature.) Cooling the sample to −30 °C (below the temperature at which ^{1}H NMR spectroscopy showed the effects of aggregation, see above) causes both the main Me_3Si and the TMEDA CH_2-peak to split into two. (The trace signal tentatively attributed to Me_3Si in the *C*-lithiate at room temperature is not observed at this lower temperature. However, at −30 °C all peaks are noticeably broader and it seems reasonable that this already weak resonance becomes difficult to detect.) If the same sample is heated to +95 °C it is found that the Me_3Si resonance (dominant at room temperature) is completely replaced by one at high field (δ = −0.7 ppm, cf. the weak δ = −0.8 ppm signal at room temperature). In the same way as for ^{1}H NMR spectroscopic data, this encourages the view that whereas the dominant species both at and below room temperature is the *N*-lithiate, it is converted into the *C*-metallated isomer at higher temperature. While the signal for the C=N carbon centre does not move in a manner that might be expected for such a rearrangement, it should be noted that the ^{13}C NMR spectra of both (*C*-lithiated) **1-Li·$^3/_2$THF** and (*N*-lithiated) **9** (in [D_6]DMSO at room temperature) show extremely similar chemical shifts for this carbon nucleus.

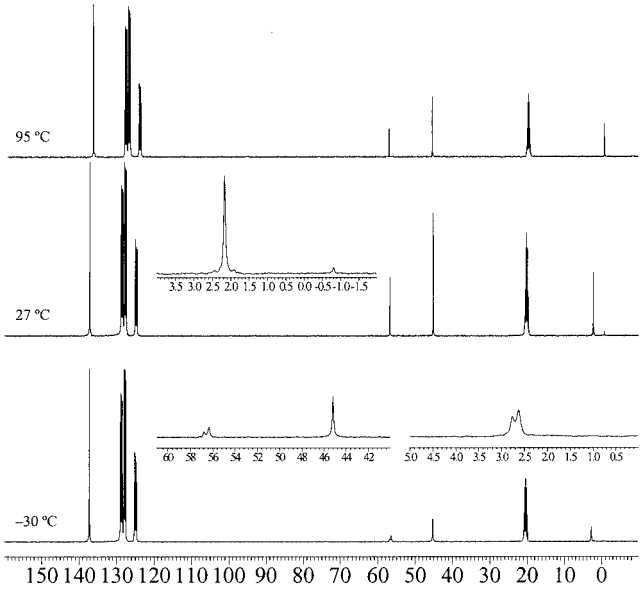

Figure 10. ^{13}C NMR spectroscopic data for **9** in [D_8]PhMe over the range 95 °C to −30 °C

Variable-temperature ^{7}Li NMR spectra (Figure 11) reinforce the information gained from ^{1}H and ^{13}C NMR spectroscopy. The single resonance observed at δ = −1.59 ppm at room temperature broadens as the temperature is lowered until at −20 °C it splits into two separate signals, consistent with the dimer-tetramer system implicated by cryoscopy. If the temperature is reduced still further this new peak becomes the dominant one. As the sample is heated to above room temperature a significant alteration in the position of the sole lithium signal can be seen. Consistent with the ^{1}H NMR spectra, this latter thermal change is irreversible.

The observation of both **1-Li·$^3/_2$THF** and **9** suggests a complicated chemistry for lithiated diazoalkanes and (in tandem with calculations) challenges previous assertions that **1-H** is necessarily preferentially *N*- rather than *C*-lithiated. Rather, calculations now suggest metallation of the carbon centre in the presence of excess donor. Indeed, further synthetic work, culminating in the isolation and structural characterisation of *N*-lithiated **9** suggests that the

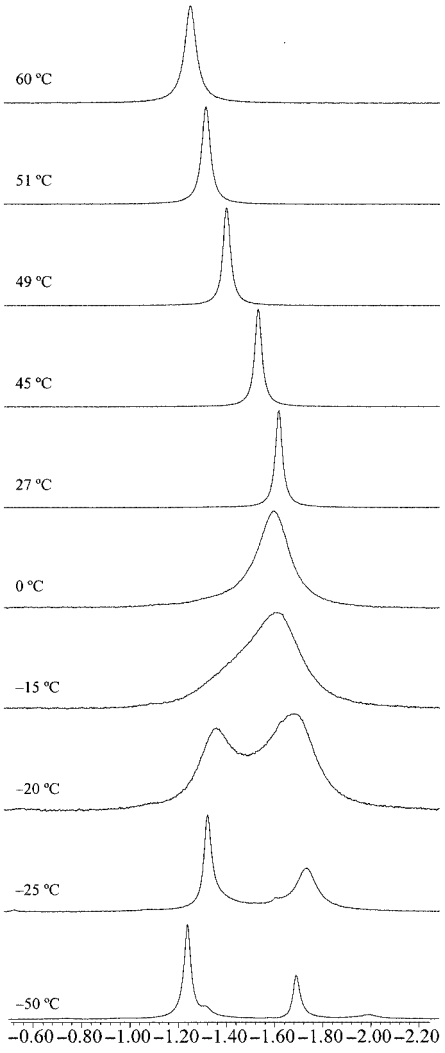

Figure 11. ^{7}Li NMR spectroscopic data for **9** in [D_8]PhMe over the range 60 °C to −50 °C

regiospecificity of metallation is temperature dependant. Clearly, such variability in the behaviour of **1-H** towards organolithium species has consequences for our understanding of the reactions undergone by the subsequently formed lithiate, and this has led us to probe the details of representative processes.

Reactions of Lithio(trimethylsilyl)diazomethane with Aryl Isothiocyanates

i) Treatment of 1-H with *n*BuLi and RNCS in THF: Syntheses of 10 (R = Ph) and 11 (R = PhCH$_2$ = Bz)

Reaction of lithio(trimethylsilyl)diazomethane with phenyl isothiocyanate (PhNCS)[18] in THF affords a product that analyses as PhNNNC(Me_3Si)C(SLi·$^3/_2$THF) **10** (Scheme 3). This shows a 1:1 Ph/Me_3Si ratio by ^{1}H NMR spectroscopy − consistent with expectation for the intended cyclised product. That ring-formation has occurred is also suggested by ^{13}C NMR spectroscopy, which reveals peaks for the sp^2 ring-carbons. However, the failure of **10** to afford crystals suitable for an unambiguous structure determination led to the replacement of phenyl isothiocyanate with its benzylic analogue (BzNCS).

Employment of BzNCS in the above reaction sequence yields a crystalline material that analyses as *S*-lithio-1-benzyl 4-trimethylsilyl-5-thio-1,2,3-triazole [BzNNNC(Me_3Si)C(SLi·2THF)], **11**. X-ray crystallography affords the first full characterisation of a lithiated thio-1,2,3-triazole (Figure 12 and Table 3; the asymmetric unit incorporates two crystallographically independent but structurally similar molecules of **11** of which a representative one is discussed). The species is rendered polymeric in the solid state through the coordination of lithium by, for example, N(3) [Li−N = 2.050(9) Å] in the almost planar (internal angles sum to 540.1°), aromatic triazole ring. The anion is formally metallated at sulfur and, at 2.460(8) Å, Li(1)−S(1) is consistent with metal-sulfur distances reported for lithium-containing thiolates,[32] thioimidates,[32j,33] and thioureas.[34] The only other solid-state structures to incorporate an alkali metallated 1,2,3-triazole ring are those of lithiated[35] and potassiated[36] benzotriazole (the triazole ring being pre-formed in both cases). In **7** a triazole ring is incorporated as a neutral adduct.[17a] The observation of a triazole ring in **11** has ramifications for our interpretation of the cyclisation process by which lithiodiazomethanes and RNCS combine to give 1-substituted 5-alkylthio-1,2,3-triazoles suggesting, as it does, the action of *C*-lithio(trimethylsilyl)diazomethane in THF solution (Scheme 4).

ii) Treatment of 1-H with *n*BuLi and RNCS in OEt$_2$: Syntheses of 12 (R = Bz) and 13 (R = Ph)

According to previous reports, the sequential combination of **1-H** with *n*BuLi and BzNCS in OEt$_2$ affords, via a postulated lithio-2-benzylamino-5-trimethylsilyl-1,3,4-thiadiazole intermediate, 2-amino-1,3,4-thiadiazoles with redirection of the reaction being attributed to an ambiguous

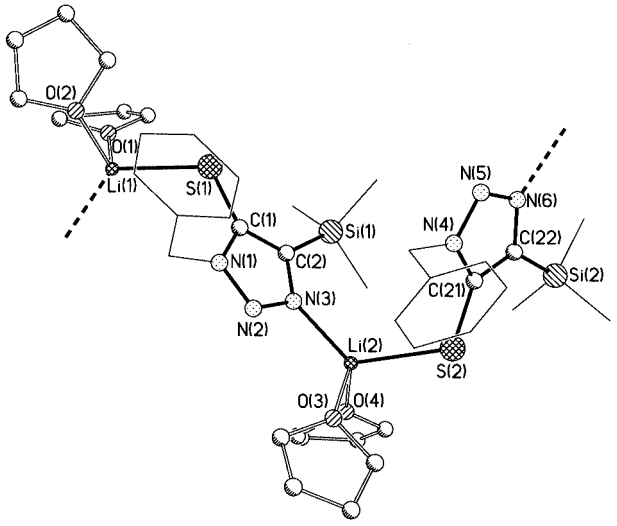

Figure 12. The solid state structure of polymeric **11**, showing the association of two crystallographically independent monomer units via *N*-stabilisation of the metal; for clarity hydrogen atoms have been omitted

Table 3. Selected bond lengths [Å] and angles [°] in **11**

Li(1)−N(6)	2.052(8)	Li(2)−N(3)	2.050(9)
Li(1)−S(1)	2.460(8)	Li(2)−S(2)	2.482(8)
S(1)−C(1)	1.717(4)	S(2)−C(21)	1.726(4)
C(1)−N(1)	1.363(5)	C(21)−N(4)	1.347(5)
C(1)−C(2)	1.383(6)	C(21)−C(22)	1.395(6)
N(1)−N(2)	1.365(5)	N(4)−N(5)	1.369(5)
N(2)−N(3)	1.314(5)	N(5)−N(6)	1.308(5)
N(3)−C(2)	1.380(5)	N(6)−C(22)	1.374(5)
S(1)−Li(1)−N(6)	124.7(4)	S(2)−Li(2)−N(3)	124.4(4)
Li(1)−S(1)−C(1)	115.8(2)	Li(2)−S(2)−C(21)	116.5(2)
N(1)−C(1)−C(2)	104.2(4)	N(4)−C(21)−C(22)	104.8(4)
C(1)−C(2)−N(3)	107.8(4)	C(21)−C(22)−N(6)	106.8(4)
C(1)−N(1)−N(2)	111.9(3)	C(21)−N(4)−N(5)	111.7(4)
N(1)−N(2)−N(3)	105.9(3)	N(4)−N(5)−N(6)	105.8(3)
N(2)−N(3)−C(2)	110.3(4)	N(5)−N(6)−C(22)	111.0(4)

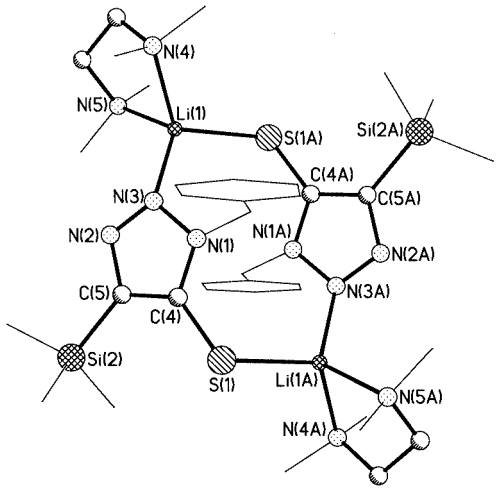

Figure 13. Molecular structure of the dimer of **12**; hydrogen atoms omitted for clarity

Table 4. Selected bond lengths [Å] and angles [°] in **12**

Li(1)−S(1A)	2.422(6)	N(1)−C(4)	1.342(4)
Li(1)−N(3)	2.053(6)	N(2)−C(5)	1.377(4)
N(3)−N(1)	1.377(4)	C(4)−C(5)	1.385(5)
N(3)−N(2)	1.285(4)	C(4)−S(1)	1.722(4)
S(1A)−Li(1)−N(3)	113.8(3)	N(1)−C(4)−C(5)	104.6(3)
Li(1)−N(3)−N(1)	124.8(3)	N(2)−C(5)−C(4)	107.7(3)
N(1)−N(3)−N(2)	107.1(3)	N(1)−C(4)−S(1)	124.0(3)
N(3)−N(1)−C(4)	110.7(3)	C(4)−S(1)−Li(1A)	111.4(2)
N(3)−N(2)−C(5)	109.9(3)		

solvent effect.[1] However, we report here that (for R = Bz) such a reaction, if followed by reflux and the addition of TMEDA affords *S*-lithio-1-benzyl 4-trimethylsilyl-5-thio-1,2,3-triazole, BzNNNC(Me_3Si)C(SLi·TMEDA) (**12**) as the only isolable product. In the solid state **12** is dimeric (Figure 13) and consists of two (mono-TMEDA) complexed metallo-1-benzyl-5-thio-4-trimethylsilyl-1,2,3-triazole molecules. Akin to **11**, **12** is an *S*-lithiate [Li−S = 2.422(6) Å], with metal centre stabilisation [Li(1)−N(3) = 2.053(6) Å] incurring dimerisation. The two planar triazole systems show aromatic character (Table 4) and, as such, are essentially similar to those in **11** notwithstanding that the N−N distances in the triazole component of **12** are consistent with greater localisation of electron density [viz. C(4)−N(1), N(1)−N(2), N(2)−N(3) in **11** and C(1)−N(1), N(1)−N(3), N(2)−N(3) in **12**]. Dimerisation of **12** results in these triazole systems being linked by (and participating in) a hitherto unknown type of 10-membered $(NNCSLi)_2$ heterocycle.

Of mechanistic importance is the observation that **12** is not the expected lithio-2-benzylamino-5-trimethylsilyl-1,3,4-thiadiazole,[1] but rather a lithio-1-benzyl 4-trimethylsilyl-5-thio-1,2,3-triazole. This is, of course, inconsistent with the reaction of *N*-lithio(trimethylsilyl)diazomethane (cf. **9**) with BzNCS but rather suggests that the reactive species in solution is the *C*-lithiate (cf. **1-Li**) instead (Scheme 4). This observation suggests several things. That the reaction is refluxed in the presence of TMEDA prior to the recrystallisation and isolation of **12** agrees with the view that preference for the *N*-lithiate is diminished in the presence of sufficiently strong external donation. Furthermore, the reaction of BzNCS with **1-Li** is apparently not facile. Hence, treatment of the lithiated diazomethane in (relatively poorly donating) OEt_2 with BzNCS at low temperature presumably gives only a slow reaction via the *N*-lithiate. However, heating of the reaction mixture immediately after introducing BzNCS (but *before* the application of TMEDA) affords the lithio-1-benzyl-5-thio-4-trimethylsilyl-1,2,3-triazole, strongly suggesting that the N-isomer has been converted into its C-congener prior to significant reaction hav-

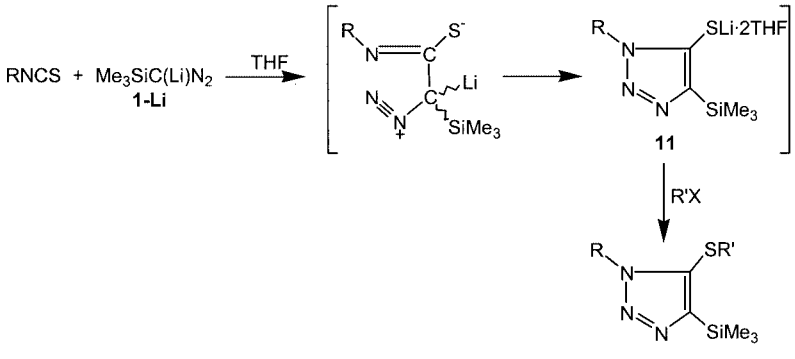

Scheme 4. Proposed mechanism for the formation of **11** from a *C*-lithiated diazomethane precursor[18]

ing occurred. Notably the synthesis of **12** can be reproduced in THF/TMEDA (with reflux prior to introduction of the bidentate donor) whereas if the literature preparation (no reflux) is closely adhered to then **1-H**, *n*BuLi and PhNCS can be sequentially combined in OEt_2 at 0 °C and worked up to give PhNHCSCHNN **13** in high yield (its formation requiring a lithio-2-phenylamino-1,3,4-thiadiazole precursor). While it has been noted that four types of cyclic system could reasonably result from the reaction of lithiodiazomethanes with aryl isothiocyanates,[37] only two such classes have been reported.[1] Reaction of the *C*-lithiate has been considered (Scheme 4) to require the initial formation of a C−C bond between the diazomethane carbanionic centre and the isothiocyanate carbon atom. However, 2-amino-5-trimethylsilyl-1,3,4-thiadiazole production necessitates that the *N*-lithio(trimethylsilyl)diazomethane molecule forms a N−C bond prior to ring closure by C−S bond formation (Scheme 5).

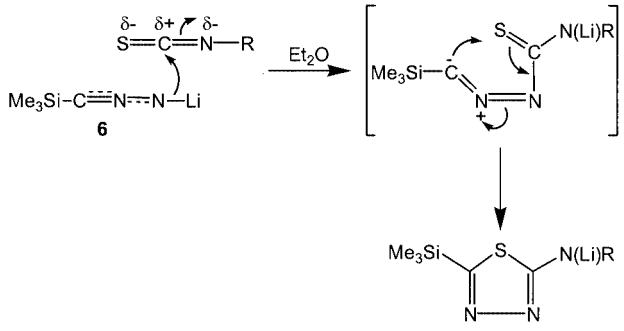

Scheme 5. Proposed mechanism for the production of lithio-2-amino-5-trimethylsilyl-1,3,4-thiadiazole from an *N*-lithiated diazomethane precursor

Conclusions

This work clearly demonstrates for the first time the viability of both the *C*- and *N*-lithiated isomers of a simple diazomethane both in the solid state (as, **1-Li·$^3/_2$THF** and **9**, respectively) and in solution. X-ray crystallographic characterisations of these two species point to bonding in the two types of molecule being quite different (Figure 14). New calculations corroborate these bonding patterns and also suggest that while the *C*-lithiated isomer of **1-Li** is less stable than its *N*-metallated analogue, the energetic difference between the two decreases with the extent of solvation by progressively stronger donors. Reaction conditions employed in the syntheses of these compounds point to the regiospecificity of metallation being significantly temperature dependent. Thus, *C*- and *N*-metallation result from the exercise of thermodynamic and kinetic control, respectively. Consistent with this is the observation, by variable temperature NMR spectroscopy, of the *irreversible* conversion of *N*- to *C*-lithiate at high temperature, a result that has significant consequences for our view of the reactivity of this lithiodiazomethane with aryl isothiocyanates.

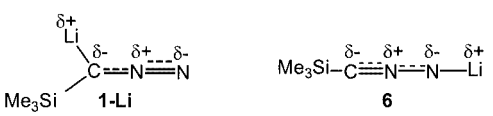

Figure 14. A review of bonding in *C*- and *N*-lithiated isomers of (trimethylsilyl)diazomethane

The solid-state structures of both **1-Li·$^3/_2$THF** and **9** indicate why it is that organic syntheses which involve the elimination of N_2 from diazomethanes require formation of the *C*-lithiate with its weak C−N and strong N=N bond. Finally, such reactivity has been probed and has resulted in the crystallographic characterisation of lithiothiotriazoles **11** and **12**. Details of their syntheses and structures bear out the view that product selectivity in these reactions, rather than being directly solvent dependent, is in fact influenced by temperature.

Experimental Section

General Remarks: All operations were carried out using standard Schlenk techniques. Toluene (freshly distilled from sodium) was added direct to the nitrogen-filled Schlenk tube using standard syringe techniques. NMR spectroscopy: Bruker DPX 250 (250.133 MHz for ^{1}H, 62.533 MHz for ^{13}C), DRX 400 (400.136 MHz for ^{1}H, 100.614 MHz for ^{13}C, 155.508 MHz for ^{7}Li), DRX 500 (500.050 MHz for ^{1}H) at 27 °C unless otherwise stated. For NMR spectroscopy, [D_6]DMSO, [D_8]THF, or [D_8]PhMe as solvents, TMS at 27 °C as external standard (for ^{1}H and ^{13}C) and PhLi in [D_8]PhMe at 27 °C as external standard (for ^{7}Li).

Synthesis of $^1/_2$[{$Me_3SiC(Li)N_2$}$_2$·3THF] (1-Li·$^3/_2$THF): Preparation as previously reported.[19] IR (Nujol): $\tilde{\nu}$ = 2149 cm^{-1} w, 2116 m (C=N=N sym. str.), 2092 m, 2052 m (C=N=N asym. str.), 838 w [$SiMe_n$ (n = 3)[38] str.], after air exposure 2160 w (C=N=N sym. str.), 2116 m (C=N=N asym. str.). ^{1}H NMR (250 MHz, [D_6]DMSO): δ = 3.60 (m, 6 H, THF), 1.76 (m, 6 H, THF), 0.05 (s, 3 H, Me), −0.18 (s, 6 H, Me) ppm. ^{13}C NMR (63 MHz, [D_6]DMSO): δ = 103.9 (C=N), 67.1 (THF), 25.2 (THF), 2.1 (SiMe), 0.4 (SiMe) ppm.

Synthesis of 6(Me_3SiCN_2Li)·2[($Me_3SiC)_2N_3Li$]·7OEt_2 [(7)$_2$·OEt_2]: Based on the literature preparation.[17a] *n*BuLi (2.5 mL, 3.2 M in hexanes, 4 mmol) was added to an OEt_2 (0.5 mL) solution of **1-H** (2 mL, 2 M in hexanes, 4 mmol) at −78 °C. The resultant orange solution was frozen in liquid nitrogen and then kept at −25 °C. Crystals of (**7**)$_2$·OEt_2 were afforded after 2 days at this temperature. The crystal structure of this compound has been reported,[17a] but supporting data has not been given previously. Yield 201 mg (30% based on **1-H**), m.p. 106−110 °C. $C_{68}H_{160}Li_8N_{18}O_7Si_{10}$ (1677): calcd. C 48.66, H 9.61, N 15.02; found C 44.93, H 9.11, N 15.34. IR (Nujol): $\tilde{\nu}$ = 2085 cm^{-1} m, 2066 m (C=N=N sym. str.), 2047 m, 2000 br (C=N=N asym. str.), 1632 m (C=C), 839 m [$SiMe_n$ (n = 3)[38] str.], after air exposure 2066 w (C=N=N sym. str.). ^{1}H NMR (500 MHz, [D_6]DMSO): δ = 3.36 (q, 15 H, OEt_2), 1.07 (t, 22.5 H, OEt_2), 0.18 (s, 36 H, Me), −0.14 (s, 12 H, Me), −0.18 (s, 42 H, Me) ppm. ^{13}C NMR (100 MHz, [D_6]DMSO): δ = 144.2 (C=C), 104.1 (C=N), 65.0 (OEt_2), 15.3 (OEt_2), 2.1 ($SiMe_3$), 0.4 ($SiMe_3$) ppm.

Synthesis of Me_3SiCN_2Li·TMEDA (9): *n*BuLi (2.5 mL, 1.6 M in hexanes, 4 mmol) was added to a TMEDA (0.9 mL, 6 mmol) solu-

tion of **1-H** (2 mL, 2 M in hexanes, 4 mmol) at −78 °C. The resultant orange solution was frozen in liquid nitrogen and then kept at −25 °C. Crystals of **9** were afforded after storage for 24 hours at this temperature. Yield 500 mg (53%), m.p. 122−124 °C. $C_{10}H_{25}LiN_4Si$ (236): calcd. C 50.82, H 10.66, N 23.70; found C 50.56, H 10.79, N 23.84. IR (Nujol): $\tilde{\nu}$ = 2129 cm^{-1} w (C=N=N sym. str.), 2042 s (C=N=N asym. str.), 835 m [$SiMe_n$ (n = 3)[38] str.], after air exposure 2171 w (C=N=N sym. str.), 2092 m (C=N=N asym. str.). ^1H NMR (400 MHz, [D_6]DMSO): δ = 2.27 (s, 4 H, CH_2), 2.11 (s, 12 H, NMe), −0.18 (s, 9 H, Me) ppm. ^{13}C NMR (100 MHz, [D_6]DMSO): δ = 104.1 (C=N), 57.0 (TMEDA), 45.6 (TMEDA), 0.3 ($SiMe_3$) ppm.

Synthesis of PhNNNC(Me_3Si)C(SLi·$^3/_2$THF) (10): nBuLi (1.25 mL, 1.6 M in hexanes, 2 mmol) was added to a THF (3.0 mL) solution of **1-H** (1 mL, 2 M in hexanes, 2 mmol) at −78 °C whereupon the solution was treated with phenyl isothiocyanate (PhNCS) (0.24 mL, 2 mmol). The orange precipitate formed on allowing the solution to warm to room temperature was dissolved at reflux and the reaction mixture was then cooled slowly to room temperature. After 1 day needles of PhNNNC(Me_3Si)C(SLi·$^3/_2$THF) (**10**) were deposited. Yield 225 mg (31%), m.p. > 116−118 °C (decomp.). $C_{34}H_{52}Li_2N_6O_3S_2Si_2$ (726): calcd. C 56.17, H 7.21, N 11.56; found C 55.82, H 7.40, N 10.46. IR (Nujol): $\tilde{\nu}$ = 2116 cm^{-1}, 2044, 1600, 1499, 1402, 1378, 839 m [$SiMe_n$ (n = 3)[38] str.], after air exposure 2053, 2028, 1625 br (C=C str.), 1499. ^1H NMR spectroscopy (400 MHz, [D_8]THF): δ = 8.12 (m, 2 H, Ph), 7.30 (m, 2 H, Ph), 7.17 (tt, 1 H, Ph), 3.59 (m, 6 H, THF), 1.75 (m, 6 H, THF), 0.33 (s, 9 H, Me) ppm. ^{13}C NMR (100 MHz, [D_8]THF): δ = 158.7 (C−S), 143.1 (C−Si), 140.7, 129.9, 128.2, 126.5, 126.1, 125.4 (Ph), −0.8 (Me) ppm.

Synthesis of BzNNNC(Me_3Si)C(SLi·2THF) (11): nBuLi (1.25 mL, 1.6 M in hexanes, 2 mmol.) was added to a THF (2.0 mL) solution of **1-H** (1 mL, 2 M in hexanes, 2 mmol) at −78 °C after which the solution was treated with benzyl isothiocyanate (BzNCS) (0.27 mL, 2 mmol). The orange precipitate formed on allowing the solution to warm to room temperature dissolved at reflux. The reaction mixture was then allowed to cool slowly to room temperature whereupon it was stored for 2 days, affording crystals of BzNNNC(Me_3Si)C(SLi·2THF) (**11**). Yield 256 mg (31%), m.p. > 168−170 °C (decomp.). $C_{20}H_{32}LiN_3O_2SSi$ (413): calcd. C 58.08, H 7.80, N 10.16; found C 57.15, H 7.76, N 10.39. IR (Nujol): $\tilde{\nu}$ = 1720 cm^{-1} w, 1403, 1217, 917, 841 [$SiMe_n$ (n = 3)[38] str.], after air exposure 1719 w, 1625 br (C=C stretch). ^1H NMR (400 MHz, [D_8]THF): δ = 7.28 (d, 2 H, Ph), 7.13 (m, 2 H, Ph), 7.08 (tt, 1 H, Ph), 5.35 (s, 2 H, CH_2), 0.29 (s, 9 H, Me) ppm. ^{13}C NMR (100 MHz, [D_8]THF): δ = 160.4 (C−S), 141.5 (C−Si), 140.2, 129.0, 128.5, 127.2 (Ph), 48.8 (CH_2), −0.8 (Me) ppm.

Preparation of BzNNNC(Me_3Si)C(SLi·TMEDA) (12): (a) nBuLi (1.25 mL, 1.6 M in hexanes, 2 mmol) was added to an OEt_2 (2.0 mL) solution of **1-H** (1 mL, 2 M in hexanes, 2 mmol) at −78 °C. BzNCS (0.27 mL, 2 mmol) was then added to the chilled solution, affording a clear yellow solution at room temperature. This was heated to reflux whereupon TMEDA (0.3 mL, 2 mmol) was added. Storage of the resultant solution for 2 days at room temperature afforded crystals of BzNNNC(Me_3Si)C(SLi·TMEDA), **12**.

(b) nBuLi (1.25 mL, 1.6 M in hexanes, 2 mmol) was added to a THF (1.8 mL) solution of **1-H** (1 mL, 2 M in hexanes, 2 mmol) at −78 °C. BzNCS (0.27 mL, 2 mmol) was then added to the chilled solution, affording a yellow precipitate at room temperature. The mixture was heated to reflux and TMEDA (0.3 mL, 2 mmol) was added, providing an orange solution. Storage of the resultant solution for 2 days at room temperature afforded crystals of **12**: Yield 154 mg (20%; route a), 62 mg (8%; route b), m.p. > 163−165 °C (decomp.). $C_{18}H_{32}LiN_5SSi$ (385): calcd. C 56.07, H 8.37, N 18.16; found C 55.99, H 8.94, N 21.43. IR (Nujol, cm^{-1}): $\tilde{\nu}$ = 1735, 1403, 1377, 842 [$SiMe_n$ (n = 3)[38] str.], after air exposure 1734, 1627 br (C=C str.), 1377. ^1H NMR (400 MHz, [D_8]THF): δ = 7.52 (d, 2 H, Ph), 7.17 (m, 2 H, Ph), 7.10 (tt, 1 H, Ph), 5.66 (s, 2 H, CH_2), 2.32 (s, 8 H, TMEDA), 2.17 (s, 24 H, TMEDA), 0.32 (s, 9 H, Me) ppm. ^{13}C NMR (100 MHz, [D_8]THF): δ = 159.9 (C−S), 140.1 (C−Si), 139.7, 128.5, 127.4, 126.0 (Ph), 57.8 (TMEDA) 47.8 (CH_2), 45.3 (TMEDA), −1.6 (Me_3Si) ppm.

Synthesis of PhNHCSCHNN (13): nBuLi (0.75 mL, 1.6 M in hexanes, 1.2 mmol) was added to an OEt_2 (10.0 mL) solution of **1-H** (0.6 mL, 2 M in hexanes, 1.2 mmol) at 0 °C. After stirring for 20 minutes PhNCS (0.12 mL, 1.2 mmol) was added to the chilled solution and the mixture stirred for a further 2 hours at this temperature. The solution was allowed to warm to room temperature and NH_4Cl (20 mL) was added. The resultant mixture was extracted with OEt_2 (2 × 10 mL) washed with water (2 × 10 mL) and dried ($MgSO_4$). Removal of excess solvent afforded **13** as a white powder. Yield 160 mg (75%), m.p. > 170−172 °C (decomp.). $C_8H_7N_3S$ (177): calcd. C 54.22, H 3.98, N 23.71; found C 53.49, H 5.43, N 21.05. IR (Nujol, cm^{-1}): $\tilde{\nu}$ = 3411, 3245 w, 3195 w (N−H str.), 1715, 1597, 1573 (C=N str.). ^1H NMR (400 MHz, [D_6]DMSO): δ = 10.42 (s, 1 H, N−H) 8.90 (s, 1 H, N=C−H), 7.65 (d, 2 H, Ph), 7.32 (m, 2 H, Ph), 7.00 (t, 1 H, Ph), 2.32 (s, 8 H, TMEDA), 2.17 (s, 24 H, TMEDA), 0.32 (s, 9 H, Me) ppm. ^{13}C NMR (100 MHz, [D_6]DMSO): δ = 164.3 (N=C(N)−S), 144.1 (S−C(H)=N), 140.8, 129.1, 121.9, 117.4 (Ph) ppm.

X-ray Crystallography: Data to check the unit cell of (**7**)$_2$·OEt_2 ($C_{68}H_{160}Li_8N_{18}O_7Si_{10}$, monoclinic, space group $C2/m$, a = 23.05, b = 15.77, c = 15.05 Å, β = 101.9°) were collected on a Rigaku R-Axis II imaging plate diffractometer[39] at 200(2)K using graphite monochromated Mo-K_α radiation (λ = 0.71069 Å). This compared with the previously published[17a] unit cell and so the full data were not collected. Data for **9** were collected on a Rigaku R-Axis II imaging plate diffractometer using 45 frames, each frame covering a 4° oscillation with an exposure time of 30 minutes per frame, in each of four orientations. Data for **11** were collected by the ω/2θ method on a Rigaku AFC-7R four circle diffractometer[39] and data for **12** were collected on a Stoe−Siemens four circle diffractometer. All structures were solved by direct methods[40] and subsequent Fourier difference syntheses and refined by full-matrix least-squares[41] on F^2 with anisotropic thermal parameters for Li, N, Si, and most C atoms. A riding model with idealised geometry was employed for H-atom refinement. For **9**, one terminal methyl group of a TMEDA molecule and three of the $SiMe_3$ groups showed positional disorder with respect to the position of the C atoms and were refined isotropically over two different sites with partial occupancies. Crystallographic data for **9**, **11** and **12** are given in Table 5. CCDC-207850 (**9**), -207849 (**11**), and -207848 (**12**) contain the supplementary crystallographic data for this paper. These data can be obtained free of charge at www.ccdc.cam.ac.uk/conts/retrieving.html [or from the Cambridge Crystallographic Data Centre, 12, Union Road, Cambridge CB2 1EZ, UK; Fax: (internat.) +44-1223/336-033; E-mail: deposit@ccdc.cam.ac.uk].

Computational Methods: Preliminary geometry optimisation calculations[20] based on XCN_2Li·nL (X = H_3Si, Me_3Si; n = 0, 1, 2; L = OEt_2, THF) were done using the 6-31G* basis set[22] at the HF level. A frequency analysis was performed on the most stable conformation of each structure and the geometry was refined using

Table 5. Crystallographic data for **9**, **11**, and **12**

	9	**11**	**12**
Formula	$C_{40}H_{100}Li_4N_{16}Si_4$	$C_{20}H_{32}LiN_3OSSi$	$C_{18}H_{32}LiN_5SSi$
M	945.48	413.58	385.58
Crystal system	Triclinic	Triclinic	Monoclinic
Space group	$P\bar{1}$	$P\bar{1}$	$C2/c$
a [Å]	14.836(2)	11.147(4)	19.705(4)
b [Å]	19.893(3)	20.679(7)	11.210(2)
c [Å]	11.880(1)	10.151(3)	23.186(5)
α [°]	99.77(1)	97.62(3)	90
β [°]	113.15(1)	90.49(4)	114.81(3)
γ [°]	84.15(1)	94.42(3)	90
U [Å^3]	3175.7(7)	2311.9(13)	4649(2)
Z	2	4	8
D_c [g cm^{-3}]	0.989	1.188	1.102
λ [Å]	0.71073	0.71069	0.71073
μ [mm^{-1}]	0.131	0.211	0.201
T [K]	180(2)	180(2)	180(2)
Refl., unique	12251, 7118	8322, 7889	4337, 4076
Refl. $F^2 > 2\sigma(F^2)$	4822	4542	2875
θ [°]	3.59−22.02	2.60−25.01	4.12−25.00
R_{int}	0.0645	0.0843	0.0567
R, $wR2$	0.0692, 0.1813	0.0707, 0.1755	0.0665, 0.1891
Parameters	606	511	235
Peak, hole [e·Å^{-3}]	0.371, −0.353	0.369, −0.304	0.839, −0.285

DFT methods (B3LYP/6-311G**).[21,22] The structural parameters reported here were taken from the DFT calculations while the electronic energy of the DFT calculation was modified by the scaled (0.91) ZPE correction taken from the HF calculation. Geometries modelled are shown in Figure 5 [XCN_2Li (X= H_3Si, Me_3Si), Me_3SiCN_2Li·L (L = OEt_2, THF)] and Figure 6 [Me_3SiCN_2Li·2 L (L = OEt_2, THF), (Me_3SiCN_2Li·TMEDA)]. The results are summarised in Table 1 and selected computed bonding parameters are given in Tables E1 and E2 (Supporting Information, see footnote on page 1 of this article).

Acknowledgments

We gratefully thank the U. K. EPSRC (R. H., M. A. H.) for financial support and Dr. Neil Feeder for collecting X-ray data for $(\mathbf{7})_2$·OEt_2, **9**, **11**, and **12**.

[1] [1a] T. Aoyama, T. Shioiri, *Tetrahedron Lett.* **1980**, *21*, 4461−4462. [1b] T. Aoyama, T. Shioiri, *Chem. Pharm. Bull.* **1981**, *29*, 3249−3255.

[2] [2a] N. Hashimoto, T. Aoyama, T. Shioiri, *Tetrahedron Lett.* **1980**, *21*, 4619−4622. [2b] N. Hashimoto, T. Aoyama, T. Shioiri, *Chem. Pharm. Bull.* **1982**, *30*, 119−124.

[3] N. Hashimoto, T. Aoyama, T. Shioiri, *Heterocycles* **1981**, *15*, 975−979.

[4] C. Baldoli, P. D. Buttero, E. Licandro, S. Maiorana, A. Papagni, A. Zanotti-Gerosa, *J. Organomet. Chem.* **1994**, *476*, C27−C29.

[5] N. Hashimoto, T. Aoyama, T. Shioiri, *Chem. Pharm. Bull.* **1981**, *29*, 1475−1478.

[6] E. W. Colvin, B. J. Hamill, *J. Chem. Soc., Perkin. Trans. 1* **1977**, 869−874.

[7] [7a] T. Aoyama, M. Kabeya, A. Fukushima, T. Shioiri, *Heterocycles* **1985**, *23*, 2363−2366. [7b] T. Aoyama, K. Sudo, T. Shioiri, *Chem. Pharm. Bull.* **1982**, *30*, 3849−3851.

[8] T. Aoyama, T. Shioiri, *Chem. Pharm. Bull.* **1982**, *30*, 3450−3452.

[9] K. Miwa, T. Aoyama, T. Shioiri, *SynLett* **1994**, 109−109.

[10] K. Miwa, T. Aoyama, T. Shioiri, *SynLett* **1994**, 107−108.

[11] R. A. Ruden, *J. Org. Chem.* **1974**, *39*, 3607−3608.

[12] H. Kai, K. Iwamoto, N. Chatani, S. Murai, *J. Am. Chem. Soc.* **1996**, *118*, 7634−7635.

[13] Y. Kita, Y. Tsuzuki, S. Kitagaki, S. Akai, *Chem. Pharm. Bull.* **1994**, *42*, 233−236.

[14] D. Seyferth, R. C. Hui, W.-L. Wang, *J. Org. Chem.* **1993**, *58*, 5843−5845.

[15] [15a] E. Müller, H. Disselhoff, *Justus Liebigs Ann. Chem.* **1934**, *512*, 250−263. [15b] E. Müller, W. Kreutzmann, *Justus Liebigs Ann. Chem.* **1934**, *512*, 264−275. [15c] E. Müller, D. Ludsteck, *Chem. Ber.* **1954**, *87*, 1887−1895. [15d] E. Müller, D. Ludsteck, *Chem. Ber.* **1955**, *88*, 921−933. [15e] E. Müller, W. Rundel, *Chem. Ber.* **1956**, *89*, 1065−1071. [15f] E. Müller, P. Kastner, R. Beutler, W. Rundel, H. Suhr, B. Zeeh, *Justus Liebigs Ann. Chem.* **1968**, *713*, 87−95. [15g] E. Müller, R. Beutler, B. Zeeh, *Justus Liebigs Ann. Chem.* **1968**, *719*, 72−79. [15h] R. Beutler, B. Zeeh, E. Müller, *Chem. Ber.* **1969**, *102*, 2636−2639.

[16] [16a] A. I. Boldyrev, P. v. R. Schleyer, A. Higgins, C. Thompson, S. S. Kamarenko, *J. Comput. Chem.* **1992**, *13*, 1066−1078. [16b] M. W. Wong, C. Wentrup, *J. Am. Chem. Soc.* **1993**, *115*, 7743−7746.

[17] [17a] G. Boche, K. Harms, M. Marsch, F. Schubert, *Chem. Ber.* **1994**, *127*, 2193−2195. [17b] G. Boche, J. C. W. Lohrenz, F. Schubert, *Tetrahedron* **1994**, *50*, 5889−5902.

[18] [18a] T. Aoyama, M. Kabeya, A. Fukushima, T. Shioiri, *Heterocycles* **1985**, *23*, 2367−2369. [18b] T. Aoyama, M. Kabeya, T. Shioiri, *Heterocycles* **1985**, *23*, 2371−2374.

[19] N. Feeder, M. A. Hendy, P. R. Raithby, R. Snaith, A. E. H. Wheatley, *Eur. J. Inorg. Chem.* **1998**, 861−864.

[20] M. J. Frisch, G. W. Trucks, H. B. Schlegel, P. M. W. Gill, B. G. Johnson, M. A. Robb, J. R. Cheeseman, T. Keith, G. A. Petersson, J. A. Montgomery, K. Raghavachari, M. A. Al-Laham, V. G. Zakrzewski, J. V. Ortiz, J. B. Foresman, J. Cioslowski, B. B. Stefanov, A. Nanayakkara, M. Challacombe, C. Y. Peng, P. Y. Ayala, W. Chen, M. W. Wong, J. L. Andres, E. S. Replogle, G. Gomperts, R. L. Martin, D. J. Fox, J. S. Brinkley, D. J. Defrees, J. Baker, J. J. P. Stewart, M. Head-Gordon, C. Gonzalez, J. A. Pople, *GAUSSIAN 94 Revision C. 3*, Gaussian, Inc., Pittsburgh, P. A., **1995**.

[21] [21a] A. D. Becke, *Phys. Rev. A* **1988**, *38*, 3098−3100. [21b] A. D. Becke, *J. Chem. Phys.* **1993**, *98*, 5648−5652.
[22] [22a] W. J. Hehre, R. Ditchfield, J. A. Pople, *J. Chem. Phys.* **1972**, *56*, 2257−2261. [22b] P. C. Hariharan, J. A. Pople, *Theor. Chim. Acta* **1973**, *28*, 213−222. [22c] J. D. Dill, J. A. Pople, *J. Chem. Phys.* **1975**, *62*, 2921−2923.
[23] [23a] R. D. Harrison, H. Ellis, *Revised Nuffield Advanced Science Book of Data*; Longman Group Ltd., Harlow, **1984**. [23b] J. G. Stark, H. G. Wallace, *Chemistry Data Book*; 2nd Edn. in SI, John Murray, London, **1992**.
[24] P. G. Williard, G. J. MacEwan, *J. Am. Chem. Soc.* **1989**, *111*, 7671−7672.
[25] N. Feeder, R. Snaith, A. E. H. Wheatley, *Eur. J. Inorg. Chem.* **1998**, 879−883.
[26] M. Pink, G. Zahn, J. Sieler, *Z. Anorg. Allg. Chem.* **1994**, *620*, 749−752.
[27] D. R. Armstrong, J. E. Davies, R. P. Davies, P. R. Raithby, R. Snaith, A. E. H. Wheatley, *New J. Chem.* **1999**, 35−41.
[28] S. R. Boss, R. Haigh, D. J. Linton, P. Schooler, G. P. Shields, A. E. H. Wheatley, *Dalton Trans.* **2003**, 1001−1008.
[29] A. J. Edwards, M. A. Paver, P. R. Raithby, C. A. Russell, D. S. Wright, *J. Chem. Soc., Dalton Trans.* **1993**, 3265−3266.
[30] C. L. Raston, B. W. Skelton, C. R. Whitaker, A. H. White, *Aust. J. Chem.* **1988**, *41*, 1925−1934.
[31] M. G. Davidson, R. Snaith, D. Stalke, D. S. Wright, *J. Org. Chem.* **1993**, *58*, 2810−2816.
[32] [32a] D. R. Armstrong, A. J. Banister, W. Clegg, W. R. Gill, *J. Chem. Soc., Chem. Commun.* **1986**, 1672−1673. [32b] A. J. Banister, W. Clegg, W. R. Gill, *J. Chem. Soc., Chem. Commun.* **1987**, 850−852. [32c] G. A. Sigel, P. P. Power, *Inorg. Chem.* **1987**, *25*, 2819−2822. [32d] K. Ruhlandte-Senge, P. P. Power, *Bull. Soc. Chim. Fr.* **1992**, *129*, 594−598. [32e] N. Frölich, P. B. Hitchcock, J. Hu, M. F. Lappert, J. R. Dilworth, *J. Chem. Soc., Dalton Trans.* **1996**, 1941−1946. [32f] K. Ruhlandte-Senge, U. Englich, M. O. Senge, S. Chadwick, *Inorg. Chem.* **1996**, *35*, 5820−5827. [32g] M. D. Janssen, E. Rijnberg, C. A. de Wolf, M. P. Hogerheide, D. Kruis, H. Kooijman, A. L. Spek, D. M. Grove, G. van Koten, *Inorg. Chem.* **1996**, *35*, 6735−6741. [32h] M. Niemeyer, P. P. Power, *Inorg. Chem.* **1996**, *35*, 7264−7272. [32i] S. Chadwick, U. Englich, K. Ruhlandte-Senge, *Organometallics* **1997**, *15*, 5792−5803. [32j] S. Chadwick, K. Ruhlandte-Senge, *Chem. Eur. J.* **1998**, *4*, 1768−1780. [32k] J. Knizek, A. Schlegel, H. Nöth, *Eur. J. Inorg. Chem.* **2001**, 181−187.
[33] [33a] H. L. van Maanen, J. T. B. H. Jastrzebski, H. Kooijman, A. L. Spek, G. van Koten, *Tetrahedron* **1994**, *50*, 11509−11526. [33b] T. Chivers, A. Downard, G. P. A. Yap, *Inorg. Chem.* **1998**, *37*, 5708−5709. [33c] T. Chivers, A. Downard, M. Parvez, *Inorg. Chem.* **1999**, *38*, 5565−5570. [33d] C. Kimblin, B. M. Bridgewater, T. Hascall, G. Parkin, *J. Chem. Soc., Dalton Trans.* **2000**, 891−897.
[34] D. R. Armstrong, R. E. Mulvey, D. Barr, R. Snaith, D. S. Wright, W. Clegg, S. M. Hodgson, *J. Organomet. Chem.* **1989**, *362*, C1−C4.
[35] C. Lambert, F. Hampel, P. v. R. Schleyer, *J. Organomet. Chem.* **1993**, *455*, 29−35.
[36] P. C. Andrews, W. Clegg, R. E. Mulvey, P. A. O'Neil, H. M. M. Wilson, *J. Chem. Soc., Chem. Commun.* **1993**, 1142−1144.
[37] M. Usher, A. Rybar, A. Martvon, J. Lesko, *Collect. Czech. Chem. Commun.* **1976**, *41*, 1182−1187.
[38] D. H. Williams, I. Fleming, *Spectroscopic Methods in Organic Chemistry*; 4th Edn., McGraw-Hill International (U. K.) Ltd., England, **1989**.
[39] *TEXSAN*, Version 1.7−1, Molecular Structure Corporation, The Woodlands, TX, **1985, 1992, 1995**.
[40] [40a] G. M. Sheldrick, *Acta Crystallogr., Sect. A* **1990**, *46*, 467−473. [40b] G. M. Sheldrick, *SHELXL-PLUS*, Program for Structure Solution and Refinement, University of Göttingen, **1991**.
[41] G. M. Sheldrick, *SHELXL-97*, Program for Crystal Structure Refinement, University of Göttingen, **1997**.

Received April 30, 2003

